The Abdus Salam
International Centre for Theoretical Physics

United Nations
Educational, Scientific
and Cultural Organization

International Atomic
Energy Agency

SMR 1673/19

AUTUMN COLLEGE ON PLASMA PHYSICS

5 - 30 September 2005

Collective Processes in Dusty Plasma Crystals

I. Kourakis
Bochum University, Germany

Collective Processes in Dusty Plasma Crystals

Ioannis Kourakis
Ruhr Universität Bochum, Institut für Theoretische Physik IV,
Fakultät für Physik und Astronomie, D-44780 Bochum, Germany
E-mail: `ioannis@tp4.rub.de`
`http://www.tp4.rub.de/∼ioannis`

Lecture Notes
Autumn College on Plasma Physics: Collective Processes
5 - 30 September 2005
Abdus Salam International Center for Theoretical Physics, Trieste, Italy

Synopsis

Plasmas, i.e. large ensembles of charged particles, consist a highly complex form of matter. From a fundamental point of view, a plasma is often modelled as a many-body system which is characterized by weak inter-particle (electrostatic) interactions (coupling). However, *strongly-coupled* charged particle configurations have recently been produced in laboratory, either by creating ultra-cold plasmas confined in a trap or by manipulating dusty plasmas in gas discharge experiments.

In this text, we aim at providing insight to the nonlinear aspects involved in the motion of charged dust grains in a one-dimensional plasma monolayer (crystal). Different types of collective excitations are reviewed, and characteristics and conditions for their occurrence in dusty plasma crystals are discussed, in a quasi-continuum approximation. Dust crystals are shown to support nonlinear kink-shaped supersonic solitary longitudinal excitations, as well as modulated envelope localized modes associated with longitudinal and transverse vibrations. Furthermore, the possibility for intrinsic localized modes (ILMs) – Discrete Breathers (DBs) – to occur is investigated, from first principles. The effect of mode-coupling is also briefly considered. The relation to previous results on atomic chains, and also to experimental results on strongly-coupled dust layers in gas discharge plasmas, is briefly discussed.

Keywords: Dusty (complex) plasmas, plasma crystals, solitons.
PACS numbers: 52.27.Lw, 05.45.Yv, 52.35.Sb

1 Introduction

Large ensembles of interacting charged particles (*plasmas*) occur in a wide variety of physical contexts, ranging from Space (solar plasmas, interplanetary matter in plasma state) and stellar environments (neutron stars, pulsars) to the Earth's atmosphere (lightnings, magnetospheric phenomena, waves in the ionosphere, noctilucent clouds) and from thermonuclear fusion reactors (*Tokamaks*) and laboratory (discharge plasmas, laser plasmas) even down to household applications (discharge light bulbs). A plasma, which is typically modeled as a collection of electrons and positive ions, is a complex physical system characterized by rich dynamics, which includes numerous collective effects (linear oscillation modes, nonlinear waves), instabilities, *etc.* Typical *e-i* plasmas are tacitly thought of as *weakly-coupled* systems, given the high temperature and low density values encountered in different natural plasma contexts [Balescu, 1988]. The strength of interparticle interactions is quantitatively expressed by the coupling parameter $\Gamma = e^2/(k_B T < r >)$, which represents the ratio of the average potential-to-kinetic energy of the charged particles; note that Γ increases (decreases) with density n (temperature T), since the mean interparticle distance $< r >\sim n^{-1/3}$ is defined as the Wigner-Seitz radius of an elementary particle sphere volume, viz. $4\pi r_{WS}^3/3 = 1/n$ (k_B denotes the Boltzmann constant). For most *e-i* plasmas of interest in space and laboratory, Γ attains very low values ($\Gamma \sim 10^{-5} - 10^{-4} \ll 1$) justifying this weak-coupling hypothesis. However, *strongly-coupled* plasmas, so far thought to exist only in exotic environments (such as neutron stars), have recently been created in laboratory, e.g. ultra-cold plasmas of laser-cooled ions, in Penning traps and storage rings (see [Killian, 2004] and Refs. therein), which freeze at ultra-low temperatures ($T \ll 1^o$ K) to form Wigner crystals, where Γ attains high values ($\Gamma > 170$ sets the theoretical crystallization limit [Ikezi, 1986]; values as high as $\Gamma \simeq 10^3 - 10^4$ are today observed in all of the systems mentioned here). A similar lattice ordering is exhibited by dusty plasmas (DP), produced during discharge plasma experiments; this exciting mesoscopic system will atract our attention in the following.

Dusty plasmas (or *complex plasmas*) consist of electrons e^- (mass m_e, charge $q_e = -e$), ions i^+ (mass m_i, charge $q_i = +Z_i e$) and massive ($M_d \simeq 10^9 m_p$, typically, where m_p is the proton mass), heavily charged ($Q_d = \pm Z_d e$, where $Z_d \simeq 10^3 - 10^4$, typically), micron-sized (typical diameter $10^{-2} - 10^2$ μm) defects, i.e. dust particulates d^- (or, less often, d^+). The presence of the latter modifies the plasma properties substantially [Verheest, 2001; Shukla & Mamun, 2002] and allows for new charged matter states, including liquid-like phases and even solid (quasi-*crystalline*) configurations [Shukla & Mamun, 2002; Morfill *et al.*, 1999; Morfill *et al.*, 2002], first realized independently by three experimental groups in 1994 [Chu & I, 1994; Hayashi & Tachibana, 1994; Thomas *et al.*, 1994].

Dust quasi-lattices are typically formed in the *sheath* region above the negative electrode in discharge plasma experiments (see in [Morfill *et al.*, 1997] for a review of the technical details and main results), and remain horizontally suspended at a levitated equilibrium position (at $z = z_0$, say) where gravity and electric (and/or magnetic [Yaroshenko, 2004]) forces mutually balance each other[1]. Typical lattice configurations include *bcc*, *fcc* and *hcp* patterns, consisting of roughly a dozen horizontal two-dimensional (2d) layers; simpler one-dimensional (1d) arrangements were also produced in laboratory, by applying appropriate confinement potentials [Misawa *et al.*, 2001; Liu *et al.*, 2003], and are thought to provide a basis for future applications.

From a fundamental point of view, these crystal-like structures are a most challenging physical system, since basic issues like the very nature of inter-particle interaction or the char-

[1] it is worth mentioning that DP lattice experiments are also currently carried out in microgravity conditions, in the International Space Station; we shall not focus in this issue here.

acteristics of oscillation modes are still being questioned. It appears to be established that electrostatic interactions (typically thought to be of screened Coulomb, i.e. Debye-Hückel type) may be strongly modified by the supersonic ion flow towards the negative electrode and the proximity of the crystal to the latter [Ignatov, 2003; Kourakis & Shukla, 2003]. Damping mechanisms due to dynamical dust charging, in addition to dust-neutral and dust-ion collisions, are some of the issues to be taken into account in a realistic description of dust crystals [Shukla & Mamun, 2002]. Interestingly, the low frequencies involved in dust lattice dynamics allow for a visualization (and digital processing) of physical phenomena on the kinetic level, in view of the study e.g. of nonlinear oscillations and waves, phase space functions (mean values), phase transitions and non-equilibrium flows, to mention only a few [Merlino et al., 1997; Thompson et al., 1999; Melandsø & Bjerkmo, 2000; Morfill *et al*, 2002]. Furthermore, notions from atomic physics are thus efficiently simulated on a more familiar mesoscopic scale[2], in an efficient (and cost affordable) manner [Maddox, 1994].

The *linear* regime of low-frequency dust grain oscillations in DP crystals, in the longitudinal (acoustic mode) and transverse (in-plane, shear mode as well as vertical, off-plane optical mode) direction(s), is now quite well understood. However, the *nonlinear* behaviour of DP crystals still remains mostly unexplored, and has lately attracted experimental [Melandsø, 1996; Nosenko et al., 2002; Nosenko et al., 2004] and theoretical interest [Melandsø, 1996; Ivlev *et al.*, 2003; Kourakis & Shukla, 2004a; b; c; d; e].

In this paper, we shall focus on the nonlinear description of dust grain displacements in a dust crystal. Considering the horizontal ($\sim \hat{x}$) and vertical (off-plane, $\sim \hat{z}$) degrees of freedom, we shall review the various nonlinear dust grain excitations occuring in a 1d dust lattice. This paper reviews relevant (more technical) theoretical studies [Kourakis & Shukla, 2004b; c; d; e]; it complements recent experimental investigations of dust crystals [Nosenko et al., 2002; Nosenko et al., 2004] and may hopefully motivate future ones. Although the results presented herein refer to mesoscopic dust crystals, they can be applied in any one-dimensional strongly-coupled lattice configuration characterized by electrostatic interactions.

2 A one-dimensional dust lattice: the model

Let us consider a quasi-1d dust layer, here assumed of infinite size, composed from identical dust grains (equilibrium charge q and mass M, both assumed constant for simplicity), located at $x_n = n\,r_0$, $(n = 0, 1, 2, ...)$. The choice of (exact form for) both the particle interaction potential $U_D(r)$ and the (anharmonic) vertical on-site potential $\Phi(z)$ will be left open (to be determined).

The Hamiltonian is of the form

$$H = \sum_n \frac{1}{2}\, M \left(\frac{d\mathbf{r}_n}{dt} \right)^2 \,+\, \sum_{m\neq n} U(r_{nm}) \,+\, \Phi_{ext}(\mathbf{r}_n)\,,$$

where $\mathbf{r}_n$ is the position vector of the $n-$th grain; $U_{nm}(r_{nm}) \equiv q\,\phi(x)$ is a binary interaction potential function related to the electrostatic potential $\phi(x)$ around the $m-$th grain, and $r_{nm} = |\mathbf{r}_n - \mathbf{r}_m|$ is the distance between the $n-$th and $m-$th grains. The external potential $\Phi_{ext}(\mathbf{r})$ accounts for the external force fields in which the crystal is embedded; in specific, Φ_{ext} takes into account the forces acting on the grains (and balancing each other at equilibrium, ensuring

[2] The typical system size is of the order of a few centimeters or less, in laboratory, while inter-particle spacing may range below or even up to 1 millimeter; the Debye radius λ_D is roughly of the same order. Dust particle temperature is approximately 300 ^{o} K, i.e. room temperature!

stability) in the vertical direction (i.e. gravity, electric and/or magnetic forces); for completeness, it might also include the confinement potential ensuring horizontal stability in experiments [Samsonov, 2002].

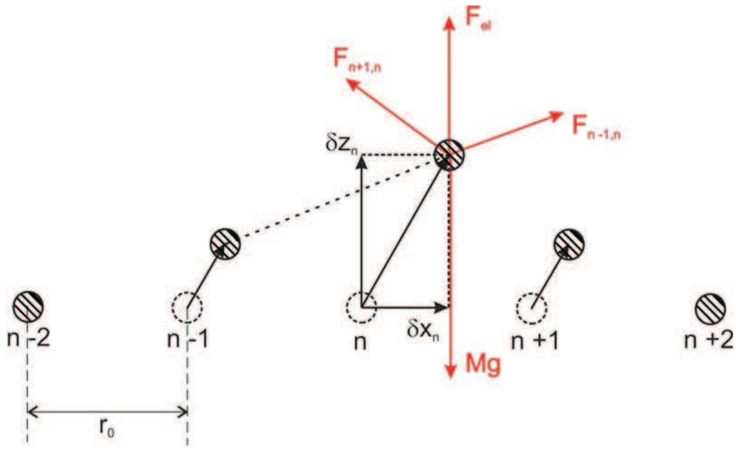

Figure 1: Dust grain vibrations in the longitudinal ($\sim \hat{x}$) and transverse ($\sim \hat{z}$) directions, in a 1d dust lattice.

2.1 2d equation of motion

Considering the motion of the $n-$th dust grain in both the *longitudinal* (horizontal, $\sim \hat{x}$) and the *transverse* (vertical, off-plane, $\sim \hat{z}$) directions (i.e. suppressing the transverse in-plane – shear – component, $\sim \hat{x}$; see Fig. 1), so that $\mathbf{r}_n = (x_n, z_n)$, we have the 2d equation of motion

$$M\left(\frac{d^2\mathbf{r}_n}{dt^2} + \nu\,\frac{d\mathbf{r}_n}{dt}\right) = -\sum_n \frac{\partial U_{nm}(r_{nm})}{\partial \mathbf{r}_n} + \mathbf{F}_{ext}(\mathbf{r}_n) \equiv q\,\mathbf{E}(\mathbf{r}_n) + \mathbf{F}_{ext}(\mathbf{r}_n)\,, \tag{1}$$

where $E_j(x) = -\partial\phi(\mathbf{r})/\partial x_j$ is the (interaction) electrostatic field and $F_{ext,j} = -\partial\Phi_{ext}(\mathbf{r})/\partial x_j$ accounts for all external forces in the j-direction ($j = 1/2$ for $x_j = x/z$); the usual *ad hoc* damping term was introduced in the left-hand-side of Eq. (1), involving the damping rate ν due to dust–neutral collisions.

2.2 Anharmonic vertical substrate potential

Assuming a smooth, continuous variation of the levitation (electric $\mathbf{E}_{ext}$ and/or magnetic $\mathbf{B}_{ext}$) field(s) and of the grain charge q (which varies due to charging processes) near the equilibrium position z_0, the electric and magnetic force(s) may be combined into an overall vertical force

$$F_{ext}(z) = F_{el/m}(z) - Mg \equiv -\partial\Phi_{ext}(z)/\partial z \approx -M[\omega_g^2\delta z_n + \alpha\,(\delta z_n)^2 + \beta\,(\delta z_n)^3] + \mathcal{O}[(\delta z_n)^4] \tag{2}$$

($\delta z_n = z_n - z_0$) where the phenomenological substrate potential $\Phi_{ext}(z)$ is of the form

$$\Phi(z) \approx \Phi(z_0) + M\left[\frac{1}{2}\omega_g^2\delta z_n^2 + \frac{\alpha}{3}\,(\delta z_n)^3 + \frac{\beta}{4}\,(\delta z_n)^4\right] + \mathcal{O}[(\delta z_n)^5]\,. \tag{3}$$

Recall that $F_{e/m}(z_0) = Mg$ at equilibrium. The gap frequency ω_g and the phenomenological anharmonicity coefficients α and β are defined via (derivatives of) $\mathbf{E}_{ext}$ and $\mathbf{B}_{ext}$ (see in [Kourakis & Shukla, 2004c; d] for the exact definitions).

The anharmonic potential $\Phi_{ext}(z)$ is depicted in Fig. 2, as it results from *ab initio* calculations [Sorasio, 2002]. It may, in priciple, be provided by experiments; see, for instance, Fig. 3.

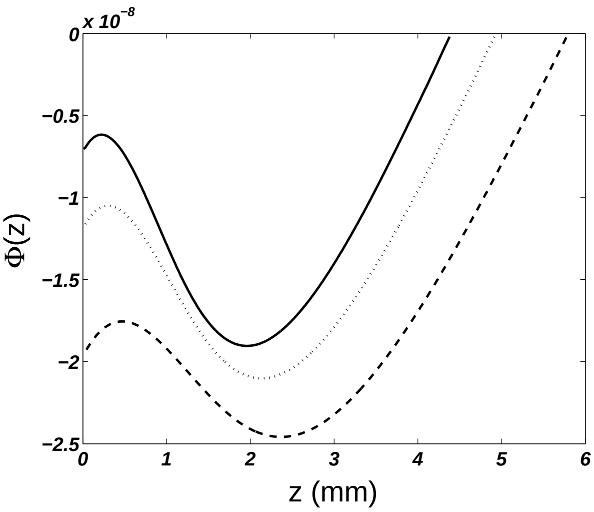

Figure 2: The (anharmonic) sheath potential $\Phi(z)$, as results from a numerical simulation of low pressure discharge experiments (data in [Sorasio, 2002]) is depicted vs. the vertical distance z from the negative electrode, for different values of the plasma particle density n (increasing from bottom to top). Note that anharmonicity is higher for lower n (bottom, dashed line), while for high n a locally parabolic form is obtained (top, solid line)(data courtesy of G. Sorasio).

2.3 Discrete equations of motion

Let $(\delta x_n, \delta z_n) = (x_n - x_n^{(0)}, z_n - z_n^{(0)})$ denote the displacement of the $n-$th grain from the equilibrium position $(x_n^{(0)}, z_n^{(0)}) = (nr_0, 0)$. Assuming small displacements from equilibrium, one may Taylor expand the interaction potential energy $U(r)$ around the equilibrium inter-grain distance $lr_0 = |n-m|r_0$ (between $l-$th order neighbors, $l = 1, 2, ...$), i.e. around $\delta x_n \approx 0$ and $\delta z_n \approx 0$, viz.

$$U(r_{nm}) = \sum_{l'=0}^{\infty} \frac{1}{l'!} \frac{d^{l'} U(r)}{dr^{l'}}\bigg|_{r=l\,|n-m|r_0} (x_n - x_m)^{l'} \,,$$

where $l' = 2$ denotes the potential parabolicity, $l' = 3$ denotes cubic nonlinearity in the interaction, and so forth. Notice that the inter-grain distance

$$r = [(x_n - x_m)^2 + (z_n - z_m)^2]^{1/2}$$

also needs to be expanded near $|x_n - x_m| = lr_0$ and $z_n - z_m = 0$, viz.

$$\frac{\partial U(r)}{\partial x_j} = \frac{\partial U(r)}{\partial r} \frac{\partial r}{\partial x_j} \approx ...$$

Retaining only nearest-neighbor interactions ($l = 1$), we obtain the coupled equations of motion

$$\begin{aligned} \frac{d^2(\delta x_n)}{dt^2} + \nu \frac{d(\delta x_n)}{dt} &= \omega_{0,L}^2 (\delta x_{n+1} + \delta x_{n-1} - 2\delta x_n) \\ &\quad - a_{20} \left[(\delta x_{n+1} - \delta x_n)^2 - (\delta x_n - \delta x_{n-1})^2 \right] \\ + a_{30} \left[(\delta x_{n+1} - \delta x_n)^3 - (\delta x_n - \delta x_{n-1})^3 \right] &+ a_{02} \left[(\delta z_{n+1} - \delta z_n)^2 - (\delta z_n - \delta z_{n-1})^2 \right] \\ - a_{12} \Big[(\delta x_{n+1} - \delta x_n)(\delta z_{n+1} - \delta z_n)^2 &- (\delta x_n - \delta x_{n-1})(\delta z_n - \delta z_{n-1})^2 \Big] \,, \end{aligned} \qquad (4)$$

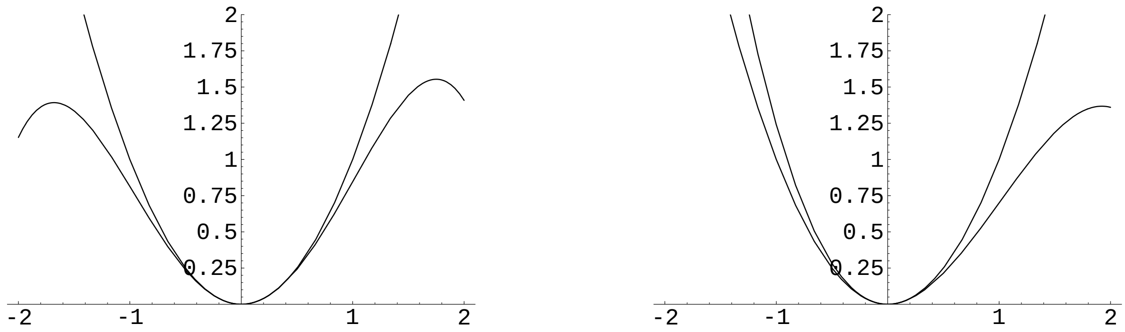

$\alpha' = +0.016$, $\beta' = -0.17$ $\qquad$ $\alpha' = -0.27$, $\beta' = -0.03$

Figure 3: The anharmonic potential $V(x)$ is depicted vs. the displacement x – see Eq. (3) – for two sets of values (corresponding to different particle size) from the Kiel experiment [Zafiu, 2001] (values adapted from Table I therein). Here, $\alpha' = \alpha r_0/\omega_g^2$ and $\beta' = \beta r_0^2/\omega_g^2$ are dimensionless parameters. The harmonic case ($\alpha' = \beta' = 0$) is also provided for reference. Note the existence of a finite potential barrier, possibly accounting for the dust crystal dissociation ("melting") reportedly observed in experiments.

and

$$\begin{aligned}\frac{d^2(\delta z_n)}{dt^2} + \nu\,\frac{d(\delta z_n)}{dt} &= \omega_{0,T}^2\,(2\delta z_n - \delta z_{n+1} + \delta z_{n-1}) \,-\, \omega_g^2\,\delta z_n \\ &\quad - \alpha\,(\delta z_n)^2 - \,\beta\,(\delta z_n)^3 + \frac{a_{02}}{r_0}\Big[(\delta z_{n+1} - \delta z_n)^3 - (\delta z_n - \delta z_{n-1})^3\Big] \\ &\quad + 2\,a_{02}\Big[(\delta x_{n+1} - \delta x_n)(\delta z_{n+1} - \delta z_n) - (\delta x_n - \delta x_{n-1})(\delta z_n - \delta z_{n-1})\Big] \\ &\quad - a_{12}\Big[(\delta x_{n+1} - \delta x_n)^2(\delta z_{n+1} - \delta z_n) - (\delta x_n - \delta x_{n-1})^2(\delta z_n - \delta z_{n-1})\Big]\,. \qquad (5)\end{aligned}$$

The longitudinal and transverse oscillation characteristic frequencies $\omega_{0,L}$ and $\omega_{0,T}$, as well as the coupling nonlinearity coefficients a_{ij}, are defined via (derivatives of) the interaction potential $U(r)$; in principle, they are positive quantities (see in the Appendix for definitions and details); in particular, such *is* the case for the Debye potential $U_D(r) = (q^2/r)\exp(-r/\lambda_D)$ (where λ_D is the effective Debye charge screening length). Recall that ω_g, α and β are related to the (anharmonic) form of the sheath potential Φ. Typical frequency values are as low as: $\omega_{0,L} \simeq 30 - 60$ sec^{-1} [Nunomura *et al.*, 2002] (i.e. $f_{0,L} = \omega_{0,L}/2\pi \approx 5 - 10$ Hz !), $\omega_{0,T} \simeq 20$ sec^{-1} and $\omega_g \simeq 160$ sec^{-1} [Misawa *et al.*, 2001], or even lower [Ivlev *et al.*, 2000; Zafiu *et al.*, 2001]. Typical values for the transverse nonlinearity coefficients may be derived from [Ivlev *et al.*, 2000][3]:

$$\alpha/\omega_g^2 \simeq -0.5\,\mathrm{mm}^{-1} \qquad \text{and} \qquad \beta \simeq 0.07\,\mathrm{mm}^{-2}\,.$$

Details on the derivation of Eqs. (4) and (5) can be found in [Kourakis & Shukla, 2004d]. As a general remark, retain that nonlinearity in dust grain dynamics in a crystals is induced by:

(a) electrostatic interactions (coupling),

(b) the plasma sheath environment (which imposes non-uniform electric/magnetic fields), and

(c) coupling between different directions of vibration (geometry).

[3]However, the strong variation from, e.g., [Zafiu *et al.*, 2001] suggests that appropriate experiments still need to be carried out before one should attempt any predictions by relying on available values.

2.4 Continuum equations of motion

Adopting the standard *continuum approximation*, one may assume that only small displacement variations occur between neighboring sites, and replace the horizontal displacement $\delta x_n(t)$ by a continuous function $u = u(x,t)$. An analogous function $w = w(x,t)$ is defined for $\delta z_n(t)$. The discrete equations of motion (4) and (5) thus lead, after a long calculation [Kourakis & Shukla, 2004d], to a set of coupled continuum equations of motion in the form

$$\ddot{u} + \nu\,\dot{u} - c_L^2\,u_{xx} - \frac{c_L^2}{12}\,r_0^2\,u_{xxxx} = -\,2\,a_{20}\,r_0^3\,u_x\,u_{xx} + 2\,a_{02}\,r_0^3\,w_x\,w_{xx}$$
$$-\,a_{12}\,r_0^4\,[(w_x)^2\,u_{xx} + 2w_x w_{xx} u_x] + 3\,a_{30}\,r_0^4\,(u_x)^2\,u_{xx}\,, \qquad (6)$$

$$\ddot{w} + \nu\,\dot{w} + c_T^2\,w_{xx} + \frac{c_T^2}{12}\,r_0^2\,w_{xxxx} + \omega_g^2\,w = -\,\alpha\,w^2 - \beta\,w^3$$
$$+\,2\,a_{02}\,r_0^3\,(u_x\,w_{xx} + w_x\,u_{xx})$$
$$+\,3\,a_{02}\,r_0^3\,(w_x)^2\,w_{xx} - a_{12}\,r_0^4\,[(u_x)^2\,w_{xx} + 2u_x u_{xx} w_x]\,, \qquad (7)$$

where higher-order nonlinear terms were omitted. We have defined the characteristic velocities $c_L = \omega_{0,L}\,r_0$ and $c_T = \omega_{0,T}\,r_0$; the subscript denotes partial differentiation, i.e. $(\cdot)_x \equiv \partial(\cdot)/\partial x$, so that $u_x\,u_{xx} = (u_x^2)_x/2$ and $(u_x)^2\,u_{xx} = (u_x^3)_x/3$.

An exact treatment of the coupled evolution Eqs. (4), (5) – or, at least, the continuum system (6), (7) – seems quite a complex task to accomplish. Even though Eq. (6) may be seen as a Boussinesq–type equation, which is now modified by the coupling, its transverse counterpart (7) substantially differs from any known nonlinear model equation. Therefore, we shall limit ourselves to reporting this coupled system of evolution equations, keeping a thorough investigation (analytical and/or numerical) of their nonlinear regime for future work. The uncoupled continuum equations (obtained upon setting either u or w to zero) will be analyzed in the following.

3 Modulated Transverse Dust Lattice Waves (TDLWs)

Let us study the vertical (off-plane) $n-$th grain displacement (i.e. for $\delta x_n = 0$), which obeys[4]

$$\frac{d^2\delta z_n}{dt^2} + \nu\,\frac{d(\delta z_n)}{dt} + \omega_{T,0}^2\,(\,\delta z_{n+1} + \delta z_{n-1} - 2\,\delta z_n) + \omega_g^2\,\delta z_n + \alpha\,(\delta z_n)^2 + \beta\,(\delta z_n)^3 = 0\,. \qquad (8)$$

Notice the difference in structure from the usual nonlinear Klein-Gordon equation used to describe 1d one-dimensional oscillator chains: transverse dust-lattice waves (TDLWs) propagating in this chain are stable *only* in the presence of the field force $F_{e/m}$ (via ω_g).

Linear transverse dust-lattice excitations, viz. $\delta z_n \sim \cos\phi_n$ (here $\phi_n = nkr_0 - \omega t$) obey the *optical*-like *discrete* dispersion relation (setting $\nu = 0$)[5]

$$\omega^2 = \omega_g^2 - 4\omega_{T,0}^2\,\sin^2\!\left(\frac{kr_0}{2}\right) \equiv \omega_T^2(k)\,. \qquad (9)$$

The TDLW dispersion curve is depicted in Fig 4. Transverse vibrations therefore propagate as a *backward wave* [see that $v_{g,T} = \omega_T'(k) < 0$] – for *any* form of $U(r)$ – in agreement with recent experiments [Misawa *et al.*, 2001]. Notice that the frequency band is limited between

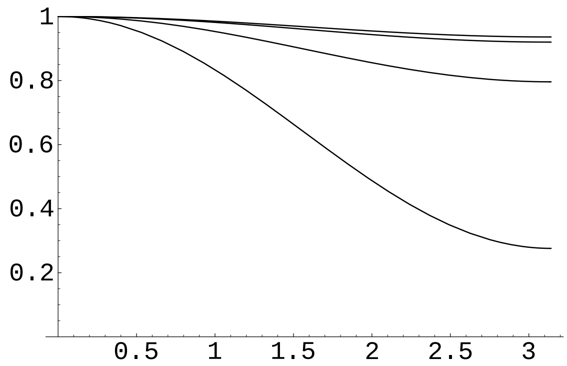

Figure 4: The dispersion relation of TDL vibrations – see Eq. Eq. (9): the frequency ω (normalized over ω_g) is depicted against the (reduced) wavenumber kr_0. The value of ω_0/ω_g ($\sim$ inter-grain coupling strength) increases from top to bottom: $\epsilon \equiv \omega_0^2/\omega_g^2 = 0.016, 0.02, 0.051, 0.181$. The uppermost (lowermost) curve, i.e. for $\epsilon = 0.016$ (0.181, respectively) correspond to the the exact experimental data in [Misawa *et al.*, 2001] ([Liu *et al.*, 2003], respectively). The upper curve(s) is (are) more likely to favor gap breathers, since the breather frequency easily satisfies the existence condition (29).

$\omega_{T,min} = (\omega_g^2 - 4\omega_{T,0}^2)^{1/2}$ (at $k = \pi/r_0$) and $\omega_{T,max} = \omega_g$, a feature which is *absent* in the continuum limit (viz. $\omega^2 \approx \omega_g^2 - \omega_0^2\, k^2\, r_0^2$, for $k \ll r_0^{-1}$).

Allowing for a slight departure from the small amplitude (linear) assumption, one may employ a multiple scale (reductive perturbation) technique to obtain, in the quasi-continuum limit[6] [Kourakis & Shukla, 2004c], the solution:

$$\delta z_n \approx \epsilon\,(A\,e^{i\phi_n} + \text{c.c.}) + \epsilon^2\,\alpha\left[-\frac{2|A|^2}{\omega_g^2} + \left(\frac{A^2}{3\omega_g^2}\,e^{2i\phi_n} + \text{c.c.}\right)\right] + \mathcal{O}(\epsilon^3)\,. \tag{10}$$

Notice the generation of higher phase harmonics due to nonlinear self-interaction. The (modulated) amplitude A obeys a *nonlinear Schrödinger* (NLS) equation in the form:

$$i\,\frac{\partial A}{\partial T} + P_T\,\frac{\partial^2 A}{\partial X^2} + Q_T\,|A|^2\,A = 0\,, \tag{11}$$

where $\{X, T\}$ are the *slow* variables $\{\epsilon(x - v_{g,L}t), \epsilon^2 t\}$. The *dispersion coefficient* P_T is related to the curvature of $\omega(k)$ as $P_T = \omega_T''(k)/2$ [to be readily computed from Eq. (9); cf. Fig. 4]. P is negative/positive for low/high values of k. The *nonlinearity coefficient*

$$Q_T = \frac{1}{2\omega_T}\left(\frac{10\alpha^2}{3\omega_g^2} - 3\,\beta\right) \tag{12}$$

may be deduced from experimental values of α and β; it turns out to be positive in (the few) known experiments on nonlinear vertical oscillation, to date [Ivlev, 2000; Zafiu, 2001].

The NLS Eq. (11) is generic: it is encountered in may physical contexts, and its behaviour has been studied since a few decades ago (see e.g. [Hasegawa, 1975; Remoissenet, 1994; Sulem, 1999]). Without going into too many details [Kourakis & Shukla, 2004c], let us summarize our current knowledge on *modulational stability* and localized solutions (*transverse envelope*

[4]The coupling anharmonicity is omitted in the right-hand side of Eq. (8), for clarity.

[5]The damping term is neglected in the following; for $\nu \neq 0$, an imaginary part appears, in account of damping, in both dispersion relation $\omega(k)$ and the resulting envelope equations.

[6]i.e. assuming a continuum variation of the amplitude, but keeping the carrier oscillation discreteness.

solitons) of Eq. (11), in the context of interest to us. In general, for $P_T Q_T < 0$, i.e. in our case (taking $Q_T > 0$) for long wavelengths $\lambda = 2\pi/k > 2\pi/k_{cr}$, or small wavenumbers $k < k_{cr}$ [where k_{cr} is the zero-dispersion-point (ZDP), defined by $\omega''(k_{cr}) = 0$], TDLWs will be modulationally stable (see in the following paragraph for details), and may propagate in the form of dark/grey envelope excitations (*hole* solitons or *voids*; see Fig. 5). On the other hand, for $P_T Q_T > 0$, i.e. here for $k > k_{cr}$ (shorter wavelengths $\lambda < 2\pi/k_{cr}$ in the first Brillouin zone), *modulational instability* may lead to the formation of bright (*pulse*) envelope solitons (see Fig. 6). Analytical expressions for these excitations can be found in [Kourakis & Shukla, 2004c], and in relevant literature [Fedele *et al.*, 2002a; b]; these expressions are briefly summarized in the following, for clarity.

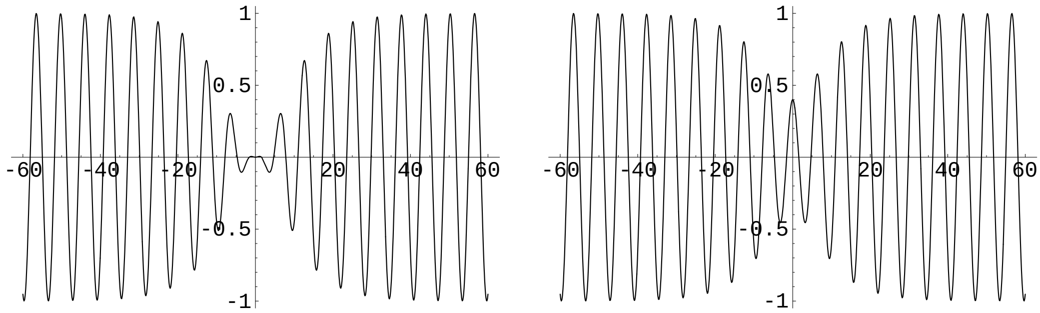

Figure 5: Envelope solitons of the (a) black, and (b) grey type.

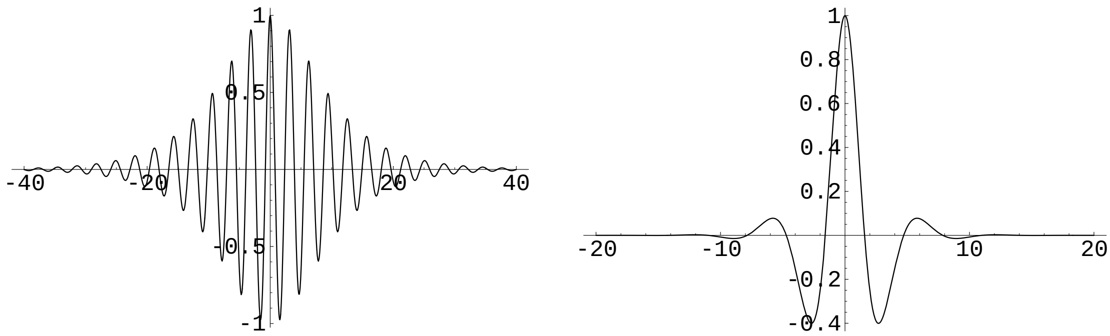

Figure 6: Envelope solitons of the bright type, for two different (arbitrary) choices of the physical parameters.

Let us note that the modulation of transverse dust grain oscillations clearly appears in numerical simulations; see e.g Fig. 9a in [Sorasio, 2002].

4 Brief Intermezzo: Modulational Instability and Soliton Solutions of the NLS Eq. (11)

For the sake of clarity, we may briefly review some of the known results on the generic NLS Equation (11). We shall denote $A = \psi$, and will drop the index T, for brevity.

4.1 Modulational (in)stability analysis

It is known (see e.g. in [Hasegawa, 1975; Remoissenet, 1994]) that the evolution of a wave whose amplitude obeys Eq. (11) depends on the coefficient product PQ, which may be investigated in terms of the physical parameters involved. To see this, first check that Eq. (11) supports the plane (Stokes') wave solution

$$\psi = \psi_0 \exp(iQ|\psi_0|^2 T)\,.$$

The standard linear analysis consists in perturbing the amplitude by setting: $\psi_0 = \hat{\psi}_0 + \epsilon\, \hat{\psi}_{1,0} \cos(\tilde{k}X - \tilde{\omega}T)$ (the perturbation wavenumber $\tilde{k}$ and the frequency $\tilde{\omega}$ should be distinguished from their carrier wave homologue quantities, denoted by k and ω). One thus obtains the (perturbation) dispersion relation:

$$\tilde{\omega}^2 \,=\, P\,\tilde{k}^2\,(P\tilde{k}^2 \,-\, 2Q|\hat{\psi}_{1,0}|^2)\,. \qquad (13)$$

One immediately sees that if $PQ > 0$, the amplitude ψ is *unstable* for $\tilde{k} < \sqrt{2Q/P}|\psi_{1,0}|$; i.e. for perturbation wavelengths larger than a critical value. If $PQ < 0$, the amplitude ψ will be *stable* to external perturbations. This *modulational instability* mechanism is tantamount to the well-known *Benjamin-Feir* instability, in hydrodynamics, and is also long recognized as an energy localization mechanism in solid state physics and nonlinear optics [Hasegawa, 1975; Remoissenet, 1994].

This type of analysis allows for a numerical investigation of the stability profile in terms of the carrier wave number k, in addition to the physical parameters involved in the problem under investigation.

4.2 Envelope excitations

The evolution equation (11) is known to be integrable; see e.g. in [Infeld & Rowlands, 1990; Remoissenet, 1994] for a presentation of the related theory. Its localized solutions, which can be rigorously obtained via the tedious Inverse Scattering Transform method, are properly speaking *solitons*, in the sense that they satisfy an infinity of conservation laws; they have been shown analytically (and confirmed numerically) to survive collisions between one another and also exhibit a robust behaviour against external perturbations.

The modulated wave resulting from the above analysis is of the form[7] $\psi = \epsilon\hat{\psi}_0' \cos(\mathbf{kr} - \omega t + \Theta) + \mathcal{O}(\epsilon^2)$, where the slowly varying amplitude $\hat{\psi}_0'$ and phase correction Θ (both real functions of $\{X, T\}$) are determined by (solving) Eq. (11) for $\psi = \psi_0 \exp(i\Theta)$; see in [Fedele *et al.*, 2002a; b] for details. Some of the different types of solution thus obtained are summarized in the following.

Bright-type envelope solitons. For *positive* PQ, the carrier wave is modulationally *unstable*; it may either *collapse*, due to (possibly random) external perturbations, or lead to the formation of *bright* envelope modulated wavepackets, i.e. localized envelope *pulses* confining the carrier (see Fig. 6):

$$\psi_0 = \left(\frac{2P}{QL^2}\right)^{1/2} \operatorname{sech}\left(\frac{X - v_e T}{L}\right), \quad \Theta = \frac{1}{2P}\left[v_e X + \left(\Omega - \frac{v_e^2}{2}\right)T\right] \qquad (14)$$

[Fedele *et al.*, 2002a; b][8], where v_e is the envelope velocity; L and Ω represent the pulse's spatial width and oscillation frequency (at rest), respectively. We note that L and ψ_0 satisfy

[7] In fact, the potential correction amplitude here is $\hat{\psi}_0' = 2\hat{\psi}_0$, from Euler's formula: $e^{ix} + e^{-ix} = 2\cos x$ ($x \in \Re$).

[8] These expressions are readily obtained from [Fedele *et al.*, 2002a; b], by shifting the variables therein to our notation as: $x \to X$, $s \to T$, $\rho_m \to \rho_0$, $\alpha \to 2P$, $q_0 \to -2PQ$, $\Delta \to L$, $E \to \Omega$, $V_0 \to u$.

$L\psi_0 = (2P/Q)^{1/2}$ = constant (in contrast with KdV solitons (see below), where $L^2\psi_0$ = const. instead). Also, the amplitude ψ_0 is independent of the pulse (envelope) velocity v_e here.

It may be pointed out that the bright (envelope) soliton phase bears a (slow) space and time dependence, thus allowing for a slight deformation of the wave packet internal structure as it propagates, whereas its envelope profile remains constant; see e.g. Fig. 7, where this effect is pointed out.

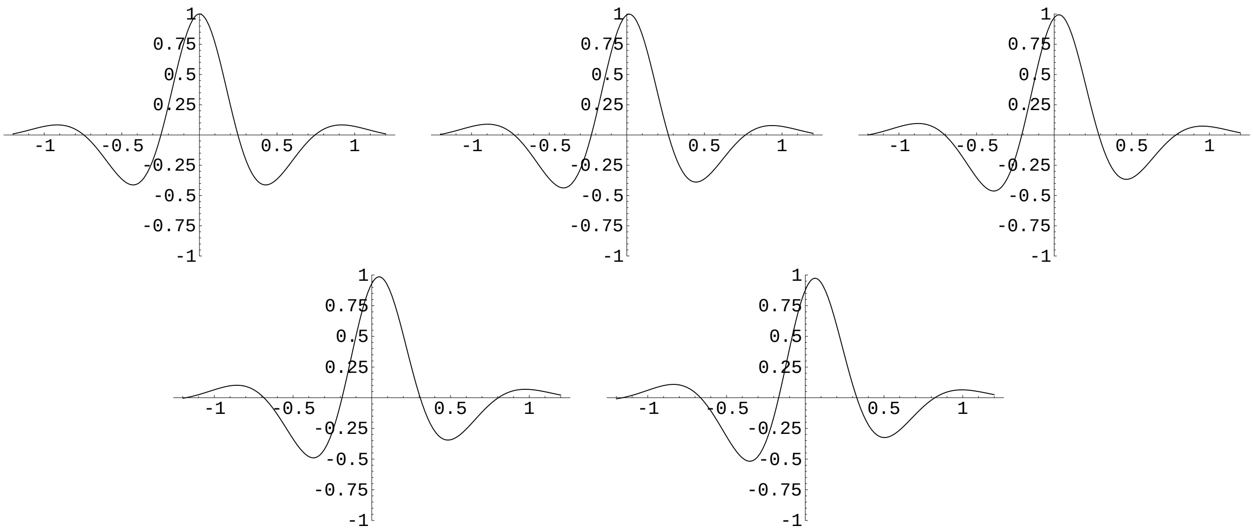

Figure 7: Bright envelope soliton propagation, at different times $t_1 < \cdots < t_5$ (arbitrary parameter values). See that, contrary to Fig. 6a (where $L \gg \lambda$), the envelope width here is comparable in order of magnitude to the carrier wavelength. Also notice the variation in internal structure, due to the (slow) phase variation in time.

Black-type envelope solitons. For $PQ < 0$, the carrier wave is modulationally *stable* and may propagate as a *dark* (*black* or *grey*) envelope wavepackets, i.e. a propagating localized *hole* (a *void*) amidst a uniform wave energy region. The exact expression for *dark* envelopes reads:

$$\psi_0 = \psi'_0 \left|\tanh\left(\frac{X - v_e T}{L'}\right)\right|, \qquad \Theta = \frac{1}{2P}[v_e X + (2PQ{\psi'_0}^2 - \frac{v_e^2}{2})T] \tag{15}$$

[Fedele *et al.*, 2002a; b][8]; see Fig. 5a. Again, $L'\psi'_0 = (2|P/Q|)^{1/2}$ (=cst.).

Grey-type envelope solitons. The *grey*-type envelope (also obtained for $PQ < 0$):

$$\psi_0 \;=\; \psi''_0 \left[1 - d^2 \,\mathrm{sech}^2\left(\frac{X - v_e T}{L''}\right)\right]^{1/2},$$

and

$$\Theta = \frac{1}{2P}\left[V_0 X - \left(\frac{1}{2}V_0^2 - 2PQ{\psi''}_0^2\right) T + \Theta_0\right] - S \sin^{-1} \frac{d \tanh(\frac{X - v_e T}{L''})}{\left[1 - d^2 \,\mathrm{sech}^2\left(\frac{X - v_e T}{L''}\right)\right]^{1/2}} \,. \tag{16}$$

Here Θ_0 is a constant phase; S denotes the product $S = \mathrm{sign}(P) \times \mathrm{sign}(v_e - V_0)$. The pulse width $L'' = (|P/Q|)^{1/2}/(d\psi''_0)$ now also depends on the real parameter d, given by:

$$d^2 \;=\; 1 \,+\, (v_e - V_0)^2/(2PQ{\psi''}_0^2) \;\leq\; 1\,.$$

The (real) velocity parameter $V_0 = \text{const.}$ satisfies [Fedele *et al.*, 2002a; b][8]:

$$V_0 - \sqrt{2|PQ|\,\psi''^2_0} \le v_e \le V_0 + \sqrt{2|PQ|\,\psi''^2_0}\,.$$

For $d = 1$ (thus $V_0 = v_e$), one recovers the *dark* envelope soliton.

5 Longitudinal Envelope Excitations

The purely longitudinal dust grain displacements $\delta x_n = x_n - nr_0$ (i.e. for $\delta z_n = 0$) are described by the nonlinear equation of motion:

$$\frac{d^2(\delta x_n)}{dt^2} + \nu\,\frac{d(\delta x_n)}{dt} = \omega_{0,L}^2\,(\delta x_{n+1} + \delta x_{n-1} - 2\delta x_n)$$
$$-a_{20}\,[(\delta x_{n+1} - \delta x_n)^2 - (\delta x_n - \delta x_{n-1})^2] + a_{30}\,[(\delta x_{n+1} - \delta x_n)^3 - (\delta x_n - \delta x_{n-1})^3]\,, \qquad (17)$$

This is reminiscent of the equation of motion in an atomic chain with anharmonic springs, that is the celebrated FPU (*Fermi-Pasta-Ulam*) problem (see e.g. in [Remoissenet, 1994] and Refs. therein).

The resulting linear mode obeys the *acoustic* dispersion relation:

$$\omega^2 = 4\omega_{L,0}^2\,\sin^2\!\left(\frac{kr_0}{2}\right) \equiv \omega_L^2(k) \qquad (18)$$

(we take $\nu = 0$ again here). The longitudinal dust-lattice wave (LDLW) dispersion curve is depicted in Fig 8.

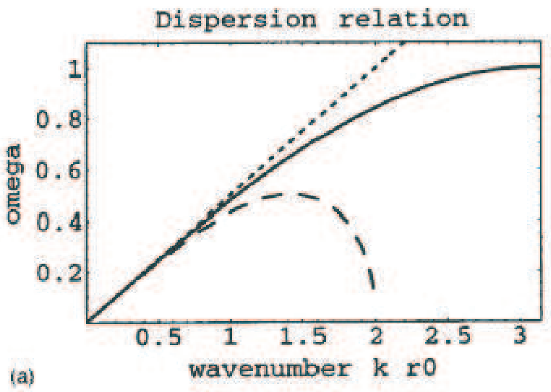

Figure 8: The longitudinal dust-lattice wave (LDLW) dispersion relation; cf. Eq. (18): frequency ω_L (normalized by $\omega_{L,0}$) vs. reduced wavenumber kr_0 (solid curve). We have also depicted: the continuous approximation (dashed curve) and the acoustic curve (tangent at the origin).

The multiple scale technique (cf. above) now yields the solution

$$\delta x_n \approx \epsilon\,[u_0^{(1)} + (u_1^{(1)}\,e^{i\phi_n} + \text{c.c.})] + \epsilon^2\,(u_2^{(2)}\,e^{2i\phi_n} + \text{c.c.}) + ... \qquad (19)$$

($\phi_n = nkr_0 - \omega t$); note the appearance (to order $\sim \epsilon$) of a *zeroth*-harmonic mode, describing a constant (center of mass) displacement in the chain. The 1st-order amplitudes obey the coupled equations [Kourakis & Shukla, 2004b]:

$$i\frac{\partial u_1^{(1)}}{\partial T} + P_L\,\frac{\partial^2 u_1^{(1)}}{\partial X^2} + Q_0\,|u_1^{(1)}|^2 u_1^{(1)} + \frac{p_0 k^2}{2\omega_L}\,u_1^{(1)}\,\frac{\partial u_0^{(1)}}{\partial X} = 0\,, \qquad (20)$$

$$\frac{\partial^2 u_0^{(1)}}{\partial X^2} = -\frac{p_0 k^2}{v_{g,L}^2 - \omega_{L,0}^2 r_0^2}\,\frac{\partial}{\partial X}\,|u_1^{(1)}|^2\,, \qquad (21)$$

where $v_{g,L} = \omega_L'(k)$; $\{X, T\}$ are the *slow* variables $\{\epsilon(x - v_{g,L}t), \epsilon^2 t\}$. The coefficients p_0 and q_0 are related to quadratic and cubic force nonlinearities (i.e. $p_0 \sim U'''(r_0)$ and $q_0 \sim U''''(r_0)$; see in the Appendix). Eqs. (20), (21) may be combined into a closed equation (for given, i.e. vanishing or constant, conditions at infinity), which is identical to Eq. (11) (setting $A \to u_1^{(1)}$ and $T \to L$ in the subscript, therein). Now, $P_L = \omega_L''(k)/2 < 0$ [to be computed from Eq. (18); cf. Fig. 8], so the form of $Q_L > 0$ (< 0) prescribes stability (instability) at low (high) k; see in [Kourakis & Shukla, 2004b] for details. The existence of the zeroth mode now results in an *asymmetric* form of the envelope excitations now obtained, namely *rarefactive bright* or *compressive dark* envelope structures; see Figs. 9, 10. In specific, in order to obtain the exact expressions for the excitations depicted in these figures, one may combine Eqs. (20) and (21) into a closed NLS Eq. in the form of Eq. (11) (for $A = u_1^{(1)}$), solve it (cf. above), and then substitute into (21) for $u_0^{(1)}$; the exact formulae thus obtained can be found in [Kourakis & Shukla, 2004b] and are therefore omitted here, for brevity.

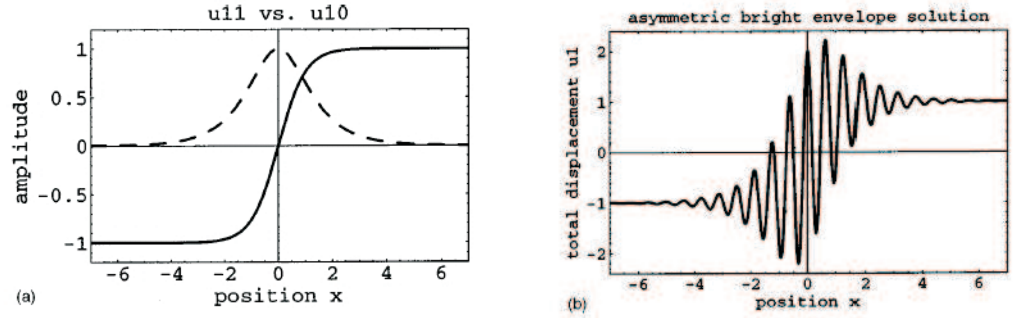

Figure 9: Bright LDL (asymmetric) envelope solitons: (a) the zeroth (pulse) and first harmonic (kink) amplitudes; (b) the resulting asymmetric wavepacket.

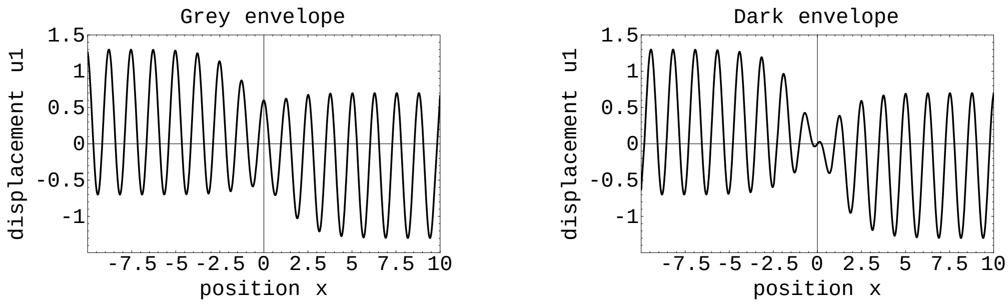

Figure 10: Dark LDL (asymmetric) modulated wavepackets of the (a) grey and (b) black type.

6 Longitudinal Solitons

Recall the (FPU) equation of motion (17), which describes the longitudinal motion of charged grains in our crystal. Inspired by methods of solid state physics, one may opt for a continuum description at a first step, viz. $\delta x_n(t) \to u(x,t)$. This may lead to different nonlinear evolution equations (depending on one's simplifying assumptions), some of which are critically discussed in [Kourakis & Shukla, 2004a]. What follows is a summary of the lengthy analysis carried out therein.

The continuum variable u obeys Eq. (6), setting $w = 0$ therein, i.e.

$$\ddot{u} + \nu\,\dot{u} - c_L^2\,u_{xx} - \frac{c_L^2}{12}\,r_0^2\,u_{xxxx} = -\,p_0\,u_x\,u_{xx} + q_0\,(u_x)^2\,u_{xx}\,, \qquad (22)$$

where the subscript denotes partial differentiation; $c_L = \omega_{L,0}\, r_0$; p_0 and q_0 are as defined above.

6.1 KdV vs. extended KdV equations

Assuming *near-sonic propagation* (i.e. $v_{sol} \approx c_L$), one obtains from Eq. (22) the *Korteweg - deVries* (KdV) equation

$$w_\tau \,-\, s\, a\, w\, w_\zeta + b\, w_{\zeta\zeta\zeta} \,=\, 0\,, \tag{23}$$

(for $\nu = 0$) in terms of the relative displacement[9] $w = u_\zeta$; here $\zeta = x - v_{sol} t$; also, $a = |p_0|/(2c_L) > 0$ and $b = c_L r_0^2/24 > 0$, while s is the sign of p_0, i.e. $s = p_0/|p_0| = \pm 1$. See that only the lowest (quadratic) order in force nonlinearity is retained here [i.e. $a \sim U'''(r_0)$].

Since the original work of Melandsø [1996], who first derived and analyzed Eq. (23) for lattice waves in Debye crystals, various studies have relied on the (abundant pre-existing knowledge on the) KdV equation[10] in order to describe the *compressive* structures subsequently sought and indeed observed in experiments [Nosenko et al., 2002; Nosenko et al., 2004]. Indeed, the KdV Eq. (23) possesses the (*negative only* here, since $a > 0$ in Debye crystals) supersonic pulse (single-)soliton solutions for w, in the form

$$w(\zeta, \tau) \,=\, -s\, w_m\, \mathrm{sech}^2\Big[(\zeta - v\tau - \zeta_0)/L_0\Big]\,, \tag{24}$$

where ζ_0 and v are arbitrary real constants. A qualitative result to be retained is the velocity dependence of both soliton amplitude $w_{1,m}$ and width L_0, viz.

$$w_m = 3v/a = 6vc_L/|p_0|\,, \qquad L_0 = (4b/v)^{1/2} = [c_L/(6v)]^{1/2} r_0\,.$$

We see that $w_m L_0^2$ = constant, implying that narrower/wider solitons are taller/shorter and faster/slower. These qualitative aspects have recently been confirmed by dust-crystal experiments [Samsonov, 2002].

Inverting back to the displacement variable $u(x,t)$, one obtains the "anti-kink" solitary wave form

$$u(x,t) \,=\, -s\, u_m\, \tanh\Big[(x - v_{sol} t - x_0)/L_1\Big]\,, \tag{25}$$

which represents a propagating localized region of compression. The amplitude u_m and the width L_1 of this shock excitation are

$$u_m \,=\, \frac{c_L r_0}{|p_0|}\, [6\, c_L\, (v_{sol} - c_L)]^{1/2}\,, \qquad L_1 \,=\, r_0 \left[\frac{c_L}{6\,(v_{sol} - c_L)}\right]^{1/2} \,=\, \frac{c_L^2 r_0^2}{|p_0|}\, \frac{1}{u_m}\,,$$

imposing 'supersonic' propagation ($v_{sol} > c_L$) for stability, in agreement with experimental results in dust crystals [Samsonov, 2002]. Note that c_L in real DP crystals is as low as a few tens of mm/sec [Samsonov, 2002; Nosenko, 2002].

Here is an important point to be made. Notice that $s = +1$ (i.e. $p_0 > 0$) if pure Debye interactions are considered (see in the Appendix). Therefore, according to the above description, the (negative pulse, for $s = +1$) KdV soliton w is interpreted as a *compressive* density variation in the crystal (see Fig. 11), viz. $n(x,t)/n_0 \sim -\partial u/\partial x \equiv -w > 0$. However, although laser

[9] The definition of the variable w here should obviously be distinguished from (and should not be confused with) the one in Eq. (7) above.

[10] The N-soliton solutions w_N of (23) are known to satisfy an infinite set of conservation laws [Karpman, 1975; Drazin, 1989]; in particular, w_N carry a constant 'mass' $M \sim \int w d\zeta$ (which is negative for a negative pulse), 'momentum' $P \sim \int w^2 d\zeta$, 'energy' $P \sim \int (w_x^2/2 + u^3)\, d\zeta$, and so forth (integration is understood over the entire $x-$ axis); see e.g. Ch. 8 in [Davydov, 1985]; also [Drazin, 1989] and Refs. therein.

triggering of compressive pulses seems easier to realize in the lab, nothing *a priori* excludes the existence of *rarefactive* longitudinal excitations in dust crystals, a question which remains open for future experiments. This apparent contradiction may be raised by a more sophisticated theory, as we shall see in the following [Kourakis & Shukla, 2004d].

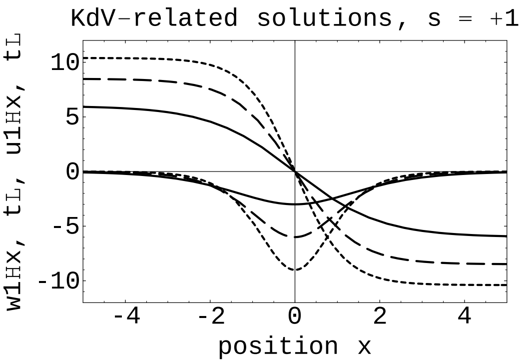

Figure 11: Localized antikink (negative pulse) solutions, as obtained from the KdV Eq. (23), for the displacement $u(x,t)$ (relative displacement $w(x,t) \sim \partial u(x,t)/\partial x$), for positive p_0, i.e. $s = +1$ (for Debye interactions); $v = 1$ (solid curve), $v = 2$ (long dashed curve), $v = 3$ (short dashed curve).

Let us see what happens if higher order nonlinearity is also kept in the description. One thus obtains the *extended KdV* (eKdV) equation

$$w_\tau - a\,w\,w_\zeta + \hat{a}\,w^2\,w_\zeta + b\,w_{\zeta\zeta\zeta} = 0\,, \tag{26}$$

where the extra coefficient $\hat{a} = q_0/(2c_L) > 0$ is related to cubic force nonlinearities [i.e. $\hat{a} \sim U''''(r_0)$]. Contrary to Eq. (23), the eKdV Eq. (26) possesses *both* negative *and* positive pulse solutions (solitons) for w, thus yielding positive *and* negative kink-shaped excitations for the displacement $u = \int w dx$; see in [Kourakis & Shukla, 2004d] for details and analytical expressions.

It is straightforward to check that $\hat{a} \simeq 2a$ roughly, in a real Debye crystal (for $\kappa \approx 1$). We thus draw the conclusion that the KdV approach is *not* sufficient. Instead, one should rather employ the *extended KdV* description, which accounts for *both* compressive *and* rarefactive lattice excitations (cf. Fig. 12), sharing the same qualitative features as its simpler KdV counterpart.

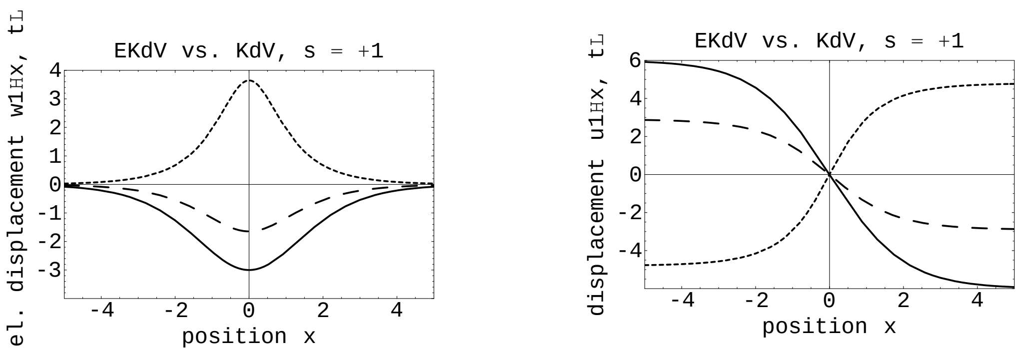

Figure 12: Solutions of the *extended* KdV Eq. (for $q_0 > 0$; dashed curves) vs. those of the KdV Eq. (for $q_0 = 0$; solid curves): (a) relative displacement u_x; (b) grain displacement u.

6.2 Boussinesq and Generalized Boussinesq equations

As an alternative to the approach presented in the previous paragraph, Eq. (22) can be reduced to a *Generalized Boussinesq* (GBq) Equation

$$\ddot{w} - v_0^2 \, w_{xx} = h \, w_{xxxx} + p \, (w^2)_{xx} + q \, (w^3)_{xx} \tag{27}$$

($w = u_x$; $p = -p_0/2 < 0$, $q = q_0/3 > 0$). For $q \sim q_0 = 0$, one recovers the *Boussinesq* (Bq) equation, widely studied in atomic chains (and hydrodynamics, earlier). As physically expected, the GBq (Bq) equation yields, like its eKdV (KdV) counterpart, *both* compressive and rarefactive (only compressive, respectively) solutions; however, the (supersonic) propagation speed v now does *not* have to be close to the sound velocity c_L (as in the KdV/eKdV cases). In any case, all of the above theories share a qualitative soliton feature, namely the decrease of the soliton width for higher velocity: the faster the soliton, the narrower it is; see Fig. 13 (also cf. Fig. 11).

A detailed comparative study of (and analytical expressions for) these soliton excitations (omitted since too lengthy to reproduce here) can be found in [Kourakis & Shukla, 2004a].

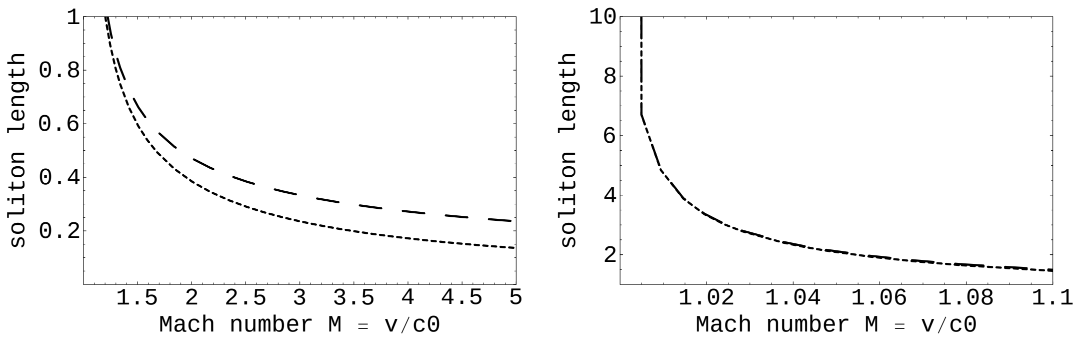

Figure 13: The (reduced) soliton length L/r_0 is depicted vs. the soliton Mach number $M = v/c_0$, as results from the GBq and the EKdV theories: lower (short-dashed) and upper (long-dashed) curves, respectively. The right figure depicts the near-sonic region, i.e. near $M = 1$, where the two theories practically coincide.

7 Intrinsic Localized Modes

Increasing interest has been manifested in the last decade in highly localized periodic nonlinear excitations occurring in discrete lattices; these *Intrinsic Localized Modes* (ILMs) were later termed *Discrete Breathers* (DBs), due to their "breathing" oscillatory character; their form reads:

$$u_n(t) = \sum_{k=-\infty}^{\infty} A_{n,k} \exp(ik\omega t) \, , \tag{28}$$

where one assumes $A_n(k) = A_n^*(-k)$ for reality and $|A_n(k)| \to 0$ as $n \to \pm\infty$, for localization. Thanks to the substrate or coupling nonlinearity (which induces an amplitude-dependence in the oscillation frequencies) and to the crystal discreteness (resulting in a finite phonon frequency band), DBs have been proved (and, lately, experimentally confirmed, in various systems) to be remarkably long-lived and robust, with respect to external perturbations; see in [Campbell *et al.*, 2004] for an introductory level review; also see [Flach & Willis, 1998] for a more exhaustive account. One might therefore naturally anticipate the existence of DBs in a dust crystal, which is intrinsically gifted with the two ingredients of the recipe: discreteness and nonlinearity.

Following the pioneering analytical and numerical considerations of ILM existence due to coupling anharmonicity (in discrete FPU chains) by Sievers, Takeno, Page and coworkers [Sievers & Takeno, 1988; Takeno & Sievers, 1988; 1989; Page, 1990] presented in the late 1980's (also see [Kiselev *et al.*, 1995; Bickham *et al.*, 1997] for a review), the existence of DB modes has been rigorously proven in the past, for a wide class of nonlinear discrete lattices. Two main axes of proof have been suggested so far, namely: (i) the analytic continuation from the uncoupled (*"anti-continuous"*) limit to a weakly interacting oscillator chain [MacKay & Aubry, 1994; Aubry, 1997], and (ii) the relation of DB existence to (intersection points of) the homoclinic orbits in the phase space defined by the Fourier component amplitudes $\{A_{nk}\}$ [Flach, 1995] (also see [Bountis, 2000]). As a matter of fact, (i) supposes (and depends on) the existence of nonlinear oscillatory solutions in the anti-continuous limit, and is thus applicable *only* in systems where nonlinearity is induced by an anharmonic on-site (substrate) potential, and where linear waves obey an *optical* dispersion law (i.e. *not* in simpler chains of nonlinearly coupled oscillators, characterized by an *acoustic* mode). The main idea of Aubry *et al.* was later revisited by Koukouloyannis & Ichtiaroglou [2002] who used a different continuation approach (based on a method dating back to the work of Poincaré; see in the latter Ref.). Technique (ii) does not imply such an assumption, and thus applies in acoustic lattices as well. A recent original formal proof of DB existence in FPU systems [James, 2001] is also worth noting.

In a general manner, the existence of DBs in a system relies on the condition:

$$n\,\omega_B \neq \omega(k)\,, \qquad\qquad \forall n \in \mathcal{N} \tag{29}$$

implying the (physically transparent) constraint that the breather frequency ω_B (and its multiples $n\omega_B$) should not enter into resonance with the linear frequency $\omega(k)$ (a function of the wavenumber k); otherwise, breather localization and longevity is destroyed, since energy is inevitably distributed among a variety of linear modes.

7.1 Discrete localized oscillations in the transverse direction

Our basis will be Eq. (8), which governs transverse vibrations in our crystal. From first principles, the existence of DBs related to transverse grain vibrations in dust lattices seems to be an inevitable reality. First, the discrete TDLW dispersion relation (9) generally predicts a very narrow frequency band $[\omega_{T,min}, \omega_{T,max}]$, since the two limit frequencies $\omega_{T,max} = \omega_g$ and $\omega_{T,min} = (\omega_g^2 - 4\omega_0^2)^{1/2}$ (see Fig. 4) are very close, in dust crystal experiments; e.g. $\omega_g \simeq 155\,\mathrm{sec}^{-1}$ and $\omega_{T,min} \simeq 150\,\mathrm{sec}^{-1}$ (derived from Fig. 3a in [Misawa, 2001]), viz. $\omega_{T,0} \simeq 20\,\mathrm{sec}^{-1}$; note that $\omega_{T,0}^2/\omega_g^2 \simeq 0.016$, implying a very weak coupling. The non-resonance condition (29) is therefore easily fulfilled, in principle. Now, the form of the on-site potential $\Phi(z)$ defined in (3) – to be in principle provided by experiments – suggests a high anharmonicity, characterized by a finite cubic term (due to its obvious asymmetry (cf. Fig. 2); for instance, the experiment by Ivlev [2000] provides: $\alpha/\omega_g^2 = -0.5\,\mathrm{mm}^{-1}$ and $\beta/\omega_g^2 = 0.07\,\mathrm{mm}^{-2}$ (for a lattice spacing, say typically, of the order of $r_0 \approx 0.5 - 1.5\,\mathrm{mm}$). Note that the damping coefficient ν therein was very low: $\nu/2\pi \simeq 0.067\,\mathrm{sec}^{-1}$ and $\omega_g/2\pi \simeq 17\,\mathrm{sec}^{-1}$, so that $\nu/\omega_g \simeq 0.004$. Similar data can be obtained from [Zafiu, 2001; Liu, 2003], although the respective experiments studied single-grain oscillations (and thus provide no information e.g. on inter-grain coupling, under the given plasma conditions).

A first approach (to be extendedly reported elsewhere) relies on the discrete NLS (DNLS) equation [Eilbeck & Johansson, 2003], which can be derived from Eq. (8) in the weak-coupling limit:

$$i \frac{du_n}{dt} + P\left(u_{n+1} + u_{n-1} - 2u_n\right) + Q\,|u_n|^2\,u_n = 0\,, \tag{30}$$

where δz_n is assumed of the form $\delta z_n \approx \epsilon u_n \cos\omega_B t + \mathcal{O}(\epsilon^2)$ and the breather frequency is close to (and above) $\omega_B \simeq \omega_g$; we have defined the smallness parameter $\epsilon = \omega_{T,0}/\omega_g$, and

$$P = -\omega_0^2/(2\omega_g) < 0\,, \qquad Q = (10\alpha^2/3\omega_g^2 - 3\beta)/2\omega_g\,. \tag{31}$$

See that $P < 0$. The sign of Q, on the other hand, depends on the sheath characteristics and cannot be prescribed. As a very preliminary remark, existing experimental values for α, β seem to suggest that $Q > 0$ (see e.g. the Ivlev values in §2.3 above above)[11]; bright (dark) DBs are thus intuitively expected to exist below (above) the linear frequency band.

This method was elegantly formulated in [Morgante, 2000][12] and in preceding studies of standing waves in lattices [Kivshar & Luther-Davies, 1998], so that long known results may apply (upon modification to account for inverse dispersion). Although this is only an approximate approach to the problem, it captures the essential physics; this method describes the well-known tendency of nonlinear discrete systems towards energy localization via modulational instability [Kivshar & Peyrard, 1992; Daumont *et al.*, 1997; Peyrard, 1998], which may possibly lead to the formation of either bright (see Fig. 14) or dark (see Fig. 15; cf. [Alvarez *et al.*, 2001]) type ILMs with frequencies outside the linear TDLW band; see [Kourakis & Shukla, 2005]. Still, values for the nonlinearity parameters should be supplied by refined, appropriately designed experiments before any conclusions are drawn.

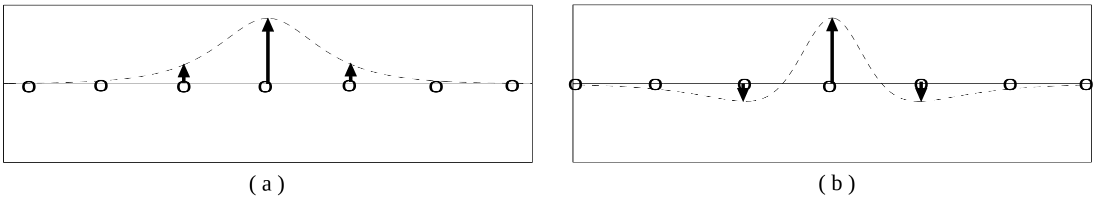

Figure 14: Localized DB excitations of the bright type (heuristic sketch): (a) odd-parity solution; (b) even-parity solution.

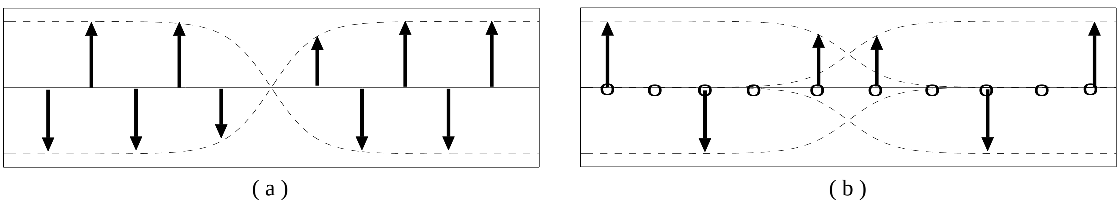

Figure 15: Localized DB excitations of the dark type (heuristic sketch): (a) black-type solution; (b) grey-type (phase-twisted) solution.

A more detailed study should incorporate a multi-mode description of transverse DBs [see Eq. (28)], via a refined analytical and numerical investigation. In specific, the requirements for (transverse) DB existence may be elegantly quantified via the frequency (square) ratio $\epsilon \equiv \omega_0^2/\omega_g^2$, which qualitatively expresses the strength of the inter-grain (electrostatic) coupling in

[11] Relying on these (preliminary) values, $\Phi(z)$ comes out to be a soft potential, i.e. nonlinear oscillation frequency will tend to lower with amplitude.

[12] see that λ therein is $\sim -Q$ here.

comparison with the substrate potential-related (single grain) oscillation eigenfrequency (see the definitions above). The limit $\epsilon \to 0$, which defines the so-called anti-continuum limit [MacKay & Aubry, 1994; Aubry, 1997], as mentioned above, describes a chain of independent oscillators (trivial localized solution). Some of the studies which are on the way regard the existence of transverse multibreathers for finite ϵ [Koukouloyannis & Kourakis, 2005], as well the exact numerical computation of such solutions via a sophisticated analytical and numerical method (which actually consists in searching for points of intersection among the homoclinic orbits in a multidimensional phase space) [Basios *et al.*, 2005]. Furthermore, at a later step, one should add effects like damping (i.e. $\nu \neq 0$) and coupling nonlinearities. These studies are on the way, and progress will be reported later.

7.2 Discrete localized oscillations in the longitudinal direction

As already mentioned, the longitudinal evolution Eq. (17) has long been studied in the context of FPU lattice theory. Following earlier pioneering works [Sievers & Takeno, 1988; Takeno & Sievers, 1988; 1989; Page, 1990] (also see in [Kiselev *et al.*, 1995; Bickham *et al.*, 1997] and Refs. therein), the existence of DBs in FPU chains was rigorously proven in [James, 2001]; see in [Sánchez-Rey *et al.*, 2004; Flach & Gorbach, 2004] for two recent studies, establishing the existence of bright and dark breathers in FPU chains. According to James [2001], small amplitude breathers with frequency slightly above the phonon band will exist if

$$B = \frac{1}{2}V''(0)V''''(0) - [V'''(0)]^2 \, > \, 0 \tag{32}$$

and will not exist otherwise. Now, expressing Eq. (17) as

$$m\frac{d^2\delta x_n}{dt^2} = V'(\delta x_{n+1} - \delta x_n) - V'(\delta x_n - \delta x_{n-1}) \, ,$$

one comes up with the effective (horizontal) coupling potential

$$V(y) = \frac{1}{2}\omega_{L,0}^2 y^2 - \frac{1}{3}a_{20}y^3 + \frac{1}{4}a_{30}y^4 \, , \tag{33}$$

which yields $B = 3a_{30}\omega_{L,0}^2 - 4a_{20}^2$ (see that B does not depend on the sign of a_{20}). Given the definitions of the coefficients $\omega_{L,0}$, a_{20} and a_{30} in our case (see in the Appendix), one may obtain B as a function of the dust lattice parameter κ, and then study it numerically: a first numerical check provides a negative B ($\forall\kappa$), hence non-existence of DBs in a (Debye) dust crystal. Of course, this conclusion depends on the form of the potential and definitely deserves further investigation (left for a more detailed report).

8 Conclusions

We have reviewed various aspects regarding the nonlinear motion of charged particles (grains) in a (1d) dust mono-layer. We have shown that the self-modulation of lattice vibrations in either the transverse or longitudinal directions, due to the sheath and electrostatic coupling nonlinearity, may lead to modulational instability and to the formation of modulated envelope localized structures (*envelope solitons*). Furthermore, localized excitations (*solitons*) may propagate in the lattice; both compressive and rarefactive longitudinal excitations (kink-shaped *solitons*) are predicted by soliton theories via a continuum approach. Finally, discrete (*breather*-type) excitations (intrinsic localized modes) may in principle occur in both longitudinal and transverse directions, provided that their frequency lies outside the linear (harmonic) frequency band.

The existence and properties of these localized excitations may be investigated (and hopefully confirmed) by appropriately designed experiments.

Acknowledgments

The author (I. K.) would like to thank the organizers of the *Autumn College on Plasma Physics: Collective Processes* (5 - 30 September 2005) for their invitation, as well as the *Abdus Salam International Center for Theoretical Physics* (ICTP, Trieste, Italy), for its hospitality.

I (I.K.) am grateful to Prof. P.K. Shukla (Ruhr Universität Bochum, Germany), who has actually co-authored the published articles where this material was drawn from.

I am also indebted to Tassos Bountis (CRANS, Univ. of Patras, Greece), Sergej Flach (MPIPKS, Dresden, Germany) and Vassilios Koukouloyannis (AUTh, Thessaloniki, Greece) for many elucidating discussions on breathers; also to Vassilios Basios (ULB, Brussels, Belgium) and Bengt Eliasson (RUB, Bochum, Germany) for numerous discussions, technical help and more. Gianfranco Sorasio (IST, GOLP, Portugal) is gratefully acknowledged for providing the numerical data for Fig. 2. Stéphane Sonmereyn (U.L.B., C.P. 165/81, Brussels, Belgium) is acknowledged for technical support.

This work was supported by the *SFB591 (Sonderforschungsbereich) – Universelles Verhalten gleichgewichtsferner Plasmen: Heizung, Transport und Strukturbildung* German government Programme.

References

Alvarez, A., Archilla, J.F.R., Cuevas J. & Romero, F.R. [2002] "Dark breathers in Klein-Gordon lattices. Band analysis of their stability properties", *New J. Phys.* **4** 72.1 - 72.19.

Aubry, S. [1997] "Breathers in nonlinear lattices: existence, linear stability and quantization", *Phys. D* **103** 201 - 250.

Balescu R. [1988] *Transport Processes in Plasmas – Volume 1: Classical transport* (North-Holland, Amsterdam).

Basios, V., Kourakis, I., Bountis, T. & Shukla, P.K. [2005], "Detection and controlability aspects of intrinsic localized modes in dusty plasma crystals, *in preparation.*

Bickham, S. R., Kiselev, S. A. & Sievers, A. J. [1997] "Intrinsic localized modes in anharmonic lattices", in *Spectroscopy and Dynamics of Collective Excitations in Solids* (B. DiBartolo, Ed.), (Plenum Press, New York), pp. 247 - 274.

Bountis, T., Capel, H.W., Kollman, M., Bergamin, J.M., Ross, J.C. & Van der Weele, J.P. "Multi-breathers and homoclinic chaos in 1-dimensional nonlinear lattices", *Phys. Lett. A* **268**, 50-60 (2000).

Campbell, D.K., Flach, S. & Kivshar, Yu.S. [2004] "Localizing energy through nonlinearity and discreteness", *Physics Today* **57** (1), 43 - 49.

Chu, J. H. & I, Lin. [1994] "Direct observation of coulomb crystals and liquids in strongly coupled RF dusty plasmas", *Phys. Rev. Lett.* **72**, 4009 - 4015.

Davydov, A.S. [1985] *Solitons in Molecular Systems* (Reidel Publ. - Kluwer, Dordrecht).

Daumont, I., Dauxois, T. & Peyrard, M. [1997] "Modulational instability: first step toward energy localization in nonlinear lattices", *Nonlinearity* **10**, 617 - 630.

Drazin, P.G. & Johnson, R.S. [1989] *Solitons: an introduction* (Cambridge Univ. Press, Cambridge U.K.).

Eilbeck, J.C. & Johansson, M. [2003] "The discrete nonlinear Schrödinger equation - 20 years on", in *Localization and Energy Transfer in Nonlinear Systems*, Eds. Vazquez, L., MacKay, R.S. & Zorzano, M.P. (World Scientific, Singapore) pp. 44-67.

Fedele, R., Schamel, H. & Shukla, P.K. [2002a] "Solitons in the Madelung's Fluid", *Phys. Scripta* T**98** 18 - 23.

Fedele, R. & Schamel, H. [2002b] "Solitary waves in the Madelung's fluid: Connection between the nonlinear Schrödinger equation and the Korteweg-de Vries equation" *Eur. Phys. J. B* **27** 313-320.

Flach, S. [1995] "Existence of localized excitations in nonlinear Hamiltonian lattices", *Phys. Rev. E* **51** 1503.

Flach, S. & Willis, C. [1998] "Discrete Breathers", *Phys. Reports* **295** 181 - 264.

Flach, S. & Gorbach, A. [2004] "Discrete breathers in Fermi-Pasta-Ulam lattices" *Chaos*, **15**, 015112; , reprint at `cond-mat/0410026`.

Hayashi, Y. & Tachibana, K. [1994] "Observation of Coulomb-Crystal Formation from Carbon Particles Grown in a Methane Plasma", *Jpn. J. Appl. Phys. Pt. 2*, **33** (6A), L804 - L806.

Hasegawa, A. [1975] *Plasma Instabilities and Nonlinear Effects* (Springer-Verlag, Berlin).

Ignatov, A. M. [2003] "Interaction between Dust Grains near a Conducting Wall", *Plasma Physics Reports* **29**, 296 - 299.

Ikezi, H. [1986] "Coulomb solid of small particles in plasmas", *Phys. Fluids* **29**, 1764 - 1766.

Infeld, E. & Rowlands, G., *Nonlinear Waves, Solitons and Chaos* (Cambridge University Press, Cambridge, England, 1990).

Ivlev, A. V., Sütterlin, R., Steinberg, V., Zuzic, M. & Morfill, G. [2000] "Nonlinear Vertical Oscillations of a Particle in a Sheath of a rf Discharge", *Phys. Rev. Lett.* **85**, 4060 - 4063.

Ivlev, A. V., Morfill, G. & Zhdanov, S. [2003] "Coupled dust-lattice solitons in monolayer plasma crystals", *Phys. Rev. E* **68**, 066402.1 - 066402.4.

James, G. [2001] "Existence of breathers on FPU lattices", *C. R. Aced. Sci. Paris* **332**, 581 - 587.

Karpman, V.I. [1975] *Nonlinear Waves in Dispersive Media* (Pergamon, New York).

Killian, T.C. [2004] "Plasmas put in order", *Nature* **429**, 815 - 816.

Kiselev, S. A., Bickham, S. R. & Sievers, A. J. [1995] "Properties of intrinsic localized modes in one-dimensional lattices", Comments on Condensed Matter Physics, **17** 135 - 173.

Kivshar, Yu. & Peyrard, M. [1992] “Modulational instabilities in discrete lattices”, *Phys. Rev. E* **46**, 3198 - 3205.

Koukouloyannis, V. & Kourakis, I. [2005] “Existence of multibreathers in the presence of an inverse dispersion law and an asymmetric on-site potential: application in transverse dusty plasma lattice oscillations, *in preparation.*

Kourakis, I. & Shukla, P.K. [2003] “Study of the intergrain interaction potential and associated instability of dust-lattice plasma oscillations in the presence of ion flow”, *Phys. Lett. A* **317** (1-2), 156 - 164.

Kourakis, I. & Shukla, P.K. [2004a] “Nonlinear theory of solitary waves associated with longitudinal particle motion in lattices: Application to longitudinal grain oscillations in a dust crystal”, *Eur. Phys. J. D* **29** (2), 247 - 263.

Kourakis, I. & Shukla, P.K. [2004b] “Modulated wavepackets associated with longitudinal dust grain oscillations in a dusty plasma crystal”, *Phys. Plasmas*, **11** (4), 1384 - 1393.

Kourakis, I. & Shukla, P.K. [2004c] “Weakly nonlinear vertical dust grain oscillations in dusty plasma crystals in the presence of a magnetic field”, *Phys. Plasmas*, **11** (7), 3665 - 3671.

Kourakis, I. & Shukla, P.K. [2004d] “Complete nonlinear theory of longitudinal-to-transverse dust lattice mode coupling in a single-layer dusty plasma crystal”, *Phys. Scripta* T**113**, 97 - 101.

Kourakis, I. & Shukla, P.K. [2005] “Discrete breather modes associated with vertical dust grain oscillations in dusty plasma crystals”, *Phys. Plasmas* **12** (1), 014502.1 - 014502.4.

Liu, B., Avinash, K. & Goree, J. [2003] “Transverse Optical Mode in a One-Dimensional Yukawa Chain”, *Phys. Rev. Lett.* **91**, 255003.

MacKay, R.S. & Aubry, S. [1994] “ Proof of existence of breathers for time-reversible or Hamiltonian networks of weakly coupled oscillators”, *Nonlinearity* **7** 1623 - 1643.

Maddox, J. [1994] “Plasma Dust as Model Crystals”, *Nature* **370** (6489), 411 - 412.

Melandsø, F. [1996] “Lattice waves in dust plasma crystals ”, *Phys. Plasmas* **3**, 3890 - 3901.

Melandsø, F. & Bjerkmo, Å. [2000] “Detection of stochastic waves in plasma monolayer crystals from video images”, *Phys. Plasmas* **7** (11), 4368 - 4378.

Merlino, R. L., Barkan, A., Thompson, C. & D’Angelo, N. [1997] *Plasma Phys. Cont. Fusion* **39**, A421 - A429.

Misawa, T., Ohno, N., Asano, K., Sawai, M., Takamura, S. & Kaw, P. K. [2001] “Experimental Observation of Vertically Polarized Transverse Dust-Lattice Wave Propagating in a One-Dimensional Strongly Coupled Dust Chain”, *Phys. Rev. Lett.* **8**6, 1219 - 1222.

Morfill, G. E., Thomas, H. M. & Zuzic, M. [1997] “Plasma crystals - a review”, in *Advances in Dusty Plasma Physics*, Eds. Shukla, P. K., Mendis, D. A. & Desai, T. (World Scientific, Singapore) pp. 99 - 142.

Morfill, G. E., Thomas, H. M., Konopka, U. & Zuzic, M. [1999] “The plasma condensation: Liquid and Crystalline plasmas”, *Phys. Plasmas* **6** (5), 1769 - 1780.

Morfill, G.E., Annaratone, B.M., Bryant, P., Ivlev, A.V., Thomas, H.M., Zuzic, M. & Fortov, V.M. [2002] “A review of liquid and crystalline plasmas: new physical states of matter?” *Plasma Phys. Cont. Fusion* **44**, B263 - B277.

Morgante, A.M., Johansson, M., Kopidakis G. & Aubry S. [2000] “Oscillatory Instabilities of Standing Waves in One-Dimensional Nonlinear Lattices”, *Phys. Rev. Lett.* **85**, 550 - 553.

Nosenko, V., Nunomura, S. & Goree, J. [2002] “Nonlinear compressional pulses in a 2D crystallized dusty plasma”, *Phys. Rev. Lett.* **88**, 215002.1 – 215002.4.

Nosenko, V., Avinash, K., Goree, J. & Liu, B. [2004] “Nonlinear Interaction of Compressional Waves in a 2D Dusty Plasma Crystal”, *Phys. Rev. Lett.* **92**, 085001.1 - 085001.4.

Nunomura, S., Goree, J., Hu, S., Wang, X. & Bhattacharjee, A. [2002] “Dispersion relations of longitudinal and transverse waves in two-dimensional screened Coulomb crystals”, *Phys. Rev. E* **65**, 066402.1 – 066402.11.

Page, J. B. [1990] “Asymptotic solutions for localized vibrational modes in strongly anharmonic periodic systems”, *Phys. Rev. B* **41**, 7835 - 7838.

Peyrard, M. [1998] “The pathway to energy localization in nonlinear lattices”, *Physica D* **119**, 184 - 199.

Remoissenet, M. [1994] *Waves Called Solitons* (Springer-Verlag, Berlin).

Samsonov, D., Ivlev, A. V., Quinn, R. A., Morfill, G. & Zhdanov, S. [2002] "Dissipative Longitudinal Solitons in a Two-Dimensional Strongly Coupled Complex (Dusty) Plasma", *Phys. Rev. Lett.* **88**, 095004.1 - 095004.4.

Sánchez-Rey, B., James, G., Cuevas, J & Archilla, J.F.R. [2004] "Bright and dark breathers in Fermi-Pasta-Ulam lattices", *Phys. Rev. B* **70**, 014301.1 - 014301.10.

Shukla, P. K. & Mamun, A. A. [2002] *Introduction to Dusty Plasma Physics* (Institute of Physics Publishing Ltd., Bristol).

Sievers, A.J. & Takeno, S. [1988] "Intrinsic Localized Modes in Anharmonic Crystals", *Phys. Rev. Lett.* **61**, 970 - 973.

Sorasio, G., Fonseca, R. A., Resendes, D. P. & Shukla, P. K. [2002] "Dust grain oscillation in plasma sheaths under low pressures" in *Dust Plasma Interactions in Space*, (Nova Publishers, New York), pp. 37 - 70.

Sulem, P. & Sulem, C. [1999] *Nonlinear Schrödinger Equation* (Springer-Verlag, Berlin).

Takeno, S. & Sievers, A.J. [1988] "Anharmonic resonant modes in perfect crystals", *Solid State Comm.* **67**, 1023 - 1026.

Takeno, S. & Sievers, A.J. [1989] "Anharmonic resonant modes and the low-temperature specific heat of glasses", *Solid State Comm.* **67**, 3374 - 3379.

Thomas, H., Morfill, G., Demmel, V., Goree, J., Feuerbacher, B. & and Möhlmann, D. [1994] "Plasma Crystal: Coulomb Crystallization in a Dusty Plasma", *Physical Review Letters* **72**, 652 - 656.

Thompson, C., Barkan, A., Merlino, R. L. & D'Angelo, N. [1999] "Video Imaging of Dust Acoustic Waves" *IEEE Trans. Plasma Sci.* **27**, 145 - 146.

Verheest, F. [2001] *Waves in Dusty Space Plasmas* (Kluwer Academic Publishers, Dordrecht).

Yaroshenko, V. V., Morfill, G. E. & Samsonov, D. [2004] "Vertical oscillations of paramagnetic particles in complex plasmas", *Phys. Rev. E* **69**, 016410.1 - 016410.5.

Zafiu, C. [2001] "Nonlinear resonances of particles in a dusty plasma sheath", *Phys. Rev. E* **63** 066403.1 - 066403.8.

Appendix

A. Definitions: characteristic frequencies and coefficients

We have defined the longitudinal/transverse oscillation characteristic frequencies

$$\omega_{0,L}^2 = U''(r_0)/M\,, \qquad \omega_{0,T}^2 = -\,U'(r_0)/(Mr_0)\,, \tag{34}$$

(both assumed to be positive for any given form of U; such *is* the case for the Debye potential: see below) and the quantities

$$a_{20} = -\frac{1}{2M}\,U'''(r_0)\,, \qquad a_{02} = -\frac{1}{2Mr_0^2}\left[U'(r_0) - r_0U''(r_0)\right]\,,$$
$$a_{30} = \frac{1}{6M}\,U''''(r_0)\,, \qquad a_{12} = -\frac{1}{Mr_0^3}\left[U'(r_0) - r_0U''(r_0) + r_0^2\,\frac{1}{2}\,U'''(r_0)\right]\,, \tag{35}$$

which are related to coupling nonlinearities. The *gap frequency* ω_g and the nonlinearity coefficients α and β are related to the form of the sheath anharmonic potential Φ via

$$\omega_g^2 = \Phi''(z_0)/M\,, \qquad \alpha = \Phi'''(z_0)/(2M)\,, \qquad \beta = \Phi''''(z_0)/(6M)\,. \tag{36}$$

The prime denotes differentiation, e.g. $U''(r_0) = d^2U(r)/dr^2\big|_{r=r_0}$.

The continuum description involves the definitions: $p_0 = -r_0^3U'''(r_0)/M \equiv 2a_{20}r_0^3$ and $q_0 = U''''(r_0)r_0^4/(2M) \equiv 3a_{30}r_0^4$; see that both are positive quantities of similar order of magnitude for Debye interactions (see in [Kourakis & Shukla, 2004a] for details).

B. Form of the coefficients for the Debye interaction potential

Consider the Debye potential (energy) $U_D(r) = q\phi_D(r) = q^2\,e^{-r/\lambda_D}/r$. Let us define the (positive real) lattice parameter $\kappa = r_0/\lambda_D$, which expresses the ratio between the lattice spacing r_0 and the Debye (screening) length λ_D. Applying the above definitions, one straightforward has

$$U_D'(r_0) = -\frac{q^2}{\lambda_D^2}\,e^{-\kappa}\,\frac{1+\kappa}{\kappa^2}\,, \qquad U_D''(r_0) = +\frac{2q^2}{\lambda_D^3}\,e^{-\kappa}\,\frac{1+\kappa+\frac{\kappa^2}{2}}{\kappa^3}\,,$$

$$U_D'''(r_0) = -\frac{6q^2}{\lambda_D^4}\,e^{-\kappa}\,\frac{1+\kappa+\frac{\kappa^2}{2}+\frac{\kappa^3}{6}}{\kappa^4}\,, \qquad U_D''''(r_0) = +\frac{24q^2}{\lambda_D^5}\,e^{-\kappa}\,\frac{1+\kappa+\frac{\kappa^2}{2}+\frac{\kappa^3}{6}+\frac{\kappa^4}{24}}{\kappa^5}\,,$$

where the prime denotes differentiation and $l = 1, 2, 3, ...$ is a positive integer. Now, combining with definitions (34, 35), we have:

$$\omega_{L,0}^2 = \frac{2q^2}{M\lambda_D^3}\,e^{-\kappa}\,\frac{1+\kappa+\kappa^2/2}{\kappa^3} \equiv c_L^2/(\kappa^2\lambda_D^2)\,, \qquad \omega_{T,0}^2 = \frac{q^2}{M\lambda_D^3}\,e^{-\kappa}\,\frac{1+\kappa}{\kappa^3} \equiv c_T^2/(\kappa^2\lambda_D^2)\,,$$

$$p_0 \equiv 2a_{20}\kappa^3\lambda_D^3 = \frac{6q^2}{M\lambda_D}\,e^{-\kappa}\left(\frac{1}{\kappa}+1+\frac{\kappa}{2}+\frac{\kappa^2}{6}\right)\,, \qquad h_0 \equiv 2a_{02}\kappa^3\lambda_D^3 = \frac{3q^2}{M\lambda_D}\,e^{-\kappa}\left(\frac{1}{\kappa}+1+\frac{\kappa}{3}\,,\right)$$

$$a_{30} = \frac{q^2}{6M\lambda_D^5}\,e^{-\kappa}\,\frac{1}{\kappa^5}\left(\kappa^4+4\kappa^3+12\kappa^2+24\kappa+24\right)\,, \qquad a_{12} = \frac{q^2}{2M\lambda_D^5}\,e^{-\kappa}\,\frac{1}{\kappa^5}\left(\kappa^3+5\kappa^2+12\kappa+12\right)\,.$$

Note that κ is of the order of unity in experiments (roughly, $\kappa \simeq 0.5 - 1.5$); therefore, all coefficients turn out to be of similar order of magnitude, as one may check numerically.

Let us retain, for later use, the characteristic dust lattice frequency scale $\omega_0 = [q^2/(M\lambda_D^3)]^{1/2}$ which naturally arises from the above definitions; in real experiments, this is of the order of XX Hz.